Vol. 71: 219–236, 2017
doi: 10.3354/cr01447

CLIMATE RESEARCH
Clim Res

Published online February 6

Future impacts of climate change on streamflows across Victoria, Australia: making use of statistical downscaling

S. Fiddes[1,2,3,*], B. Timbal[3]

[1]Australian-German Climate and Energy College, University of Melbourne, Parkville, Victoria 3010, Australia
[2]ARC Centre of Excellence for Climate System Science, School of Earth Sciences, University of Melbourne, Parkville, Victoria 3010, Australia
[3]Australian Bureau of Meteorology, 700 Collins Street, Melbourne 3001, Australia

ABSTRACT: Streamflows in key catchments across the State of Victoria, Australia, are projected into the future utilising a previously developed multiple linear regression. The regression uses a temporal range of rainfall and temperature parameters to compute monthly streamflows, and is applied to an ensemble of 22 statistically downscaled global climate models. This method reproduced historical streamflows well: on average the reconstruction overestimated the observed mean by 1% and underestimated the observed variance by 2%, although this varied on a catchment-to-catchment basis. Despite the accurate reconstruction of the mean streamflow, no events of similar magnitude to the most severe drought on record (the Millennium drought, 1997–2009) were found in the historical reconstruction for the current climate. Furthermore the reconstructed streamflow did not exhibit declining trends similar to what has been observed, due to the absence of declining rainfall in the climate model simulations for the historical record. Future projections under a high emissions pathway indicate a large reduction (24–87%) in streamflow by the end of the century, with conditions similar to the Millennium drought becoming the norm. The driest 10 yr mean streamflow was found to be 78% worse than the Millennium drought under a high emissions pathway. The greatest reductions in streamflow are seen through the May–November period. This is an important step in understanding how Victoria's water security will be affected by climate change.

KEY WORDS: Streamflow · Rainfall · Victoria, Australia · Water availability · Climate change · Climate projections · Catchment modelling

1. INTRODUCTION

Understanding the behaviour of Victoria's water catchments is of upmost importance for the state's water security, made clear by the impacts of the recent Millennium drought. This event, spanning 1997–2009, was observed to be southeast Australia's longest and most severe drought in the observational record (Timbal 2009). During this period, rainfall was 12% below the 1900–2012 mean (CSIRO 2010) and streamflow across the catchments studied in this work experienced declines of between 14 and 90% from the 1977–2012 mean (Fiddes & Timbal 2016).

With Victoria's population expected to grow to 10 million by 2051 (DTPLI 2014), water demand for domestic means, agriculture and industry are expected to increase accordingly. Current climate projections are indicating that Victoria is likely to shift to a warmer, drier climate (IPCC 2007, 2013, CSIRO & BoM 2015). This decline in rainfall could further translate to declines of up to 2 to 3 times greater in surface water (Chiew 2006, CSIRO 2012), putting further stress on the state's water management.

*Corresponding author:
sonya.fiddes@climate-energy-college.org

It has been shown that selected catchments across Victoria experienced a decline in streamflow over 1977–2012 of up to 7% on average (Fiddes & Timbal 2016). Drier catchments experienced greater declines (up to 30% in the east and west of the state), whilst wetter, alpine catchments in some cases experienced no meaningful trends. Similar trends have been reported for the Murray–Darling Basin (MDB) for a range of water indicators (Potter & Chiew 2009, CSIRO 2010, Leblanc et al. 2011).

Nonlinear processes within individual catchments cause an elasticity of the streamflow response to rainfall changes. For example, streamflow changes during the Millennium drought that were 3.4 times greater than the changes in rainfall in the same period (CSIRO 2010). Catchments of differing physical characteristics and climate (e.g. in levels of aridity), and which experience prolonged stress, respond differently to changes in rainfall (Chiew 2006, Murphy et al. 2010, CSIRO 2012, Saft et al. 2015, Fiddes & Timbal 2016).

It is essential that these processes are understood, and they should be captured when modelling streamflows at fine temporal timescales. However, at a monthly time scale, simple time-series-based linear regressions can satisfactorily reconstruct streamflows, especially those that experience flows for at least 70% of the year, whereas drier catchments are less well captured (Chiew et al. 1993). This was further confirmed using direct general circulation model (GCM) outputs and a multiple linear regression to predict monthly streamflows for a catchment in western Victoria, though there were problems predicting extremes in the streamflow time series (Sachindra et al. 2013, 2015).

A multiple linear regression using rainfall of the concurrent month, previous month and previous year, and temperature of the concurrent month was developed to reconstruct historical streamflow for Melbourne's water catchments (Timbal et al. 2015a). This method was developed further (Fiddes & Timbal 2016) by adding a long-term (10 yr) rainfall memory, and applied to 27 diverse catchments across the state. The statistical reconstructions were able to replicate the monthly streamflow time series well, with an adjusted explained variance ($\overline{R^2}$) of 88%. The mean of the time series was highly accurate, whilst streamflow variance (σ^2) was underestimated. Long-term trends were reconstructed with good skill, whilst the magnitudes of the Millennium drought event were underestimated in the worst-affected catchments. Here, the same statistical reconstruction is applied to an ensemble of statistically downscaled climate model simulations from the Coupled Model Intercomparison Project phase 5 (CMIP5) database.

Previous work investigating the performance of the CMIP5 ensembles indicates a good ability to reproduce the spatial pattern of Australian rainfall mean and interannual variability (Smith et al. 2013), whilst the variance is underestimated (Irving et al. 2012). Historical rainfall trends are not well captured (CSIRO & BoM 2015). A decline in precipitation for southeast Australia under representative concentration pathway (RCP) 8.5, especially during winter and spring, is projected; however, model agreement is not strong, and the ability to reproduce the annual cycles are conflicting (Irving et al. 2012, Smith et al. 2013, Grose et al. 2015a, Timbal et al. 2015b).

Statistical downscaling of the CMIP5 GCMs uses the relationships between local weather and large-scale climate patterns that can be inferred from GCM outputs. This method provides a GCM output of 5 km resolution, as opposed to the original GCM resolution of 150 to 400 km, providing much greater detail of rainfall and temperature patterns across the state, whilst also generally improving the GCM projections of rainfall. A similar method was used to predict point-based monthly streamflows directly from GCM output (Sachindra et al. 2013, 2015). Whilst rainfall projections from GCMs are not as reliable as, for example, temperature projections, due to its inherent variability, at monthly timescales the hydrological community generally find analysis of average rainfall and subsequent impact studies appropriate. Some examples of the application of GCM rainfall projections to hydrological studies are commented on below.

Studies projecting streamflow or runoff generally use individual catchment hydrological models of different levels of complexity, such as the Sacramento or SYMHYD models (Chiew et al. 2008, CSIRO 2012, Post & Moran 2013). These hydrological models are lumped conceptual daily rainfall–runoff models, and are driven by climate observations (rainfall and potential evaporation in these cases cited above) scaled by climate projections, in effect changing the background mean, variance or even entire distribution. This 'scaling factor', or climate change signal, remains at course resolution, unable to capture the effects of topography and coastlines on the climate variables (Chiew et al. 2008, Post & Moran 2013).

Such results for the southern MDB (encompassing northern Victoria) range from –22 to –2% changes in streamflow with 1°C of warming relative to 1990 (CSIRO 2012). A reduction of –14 and –25% was found for median climate pathways for 2030 and 2060, respectively (Post & Moran 2013). Similarly, an

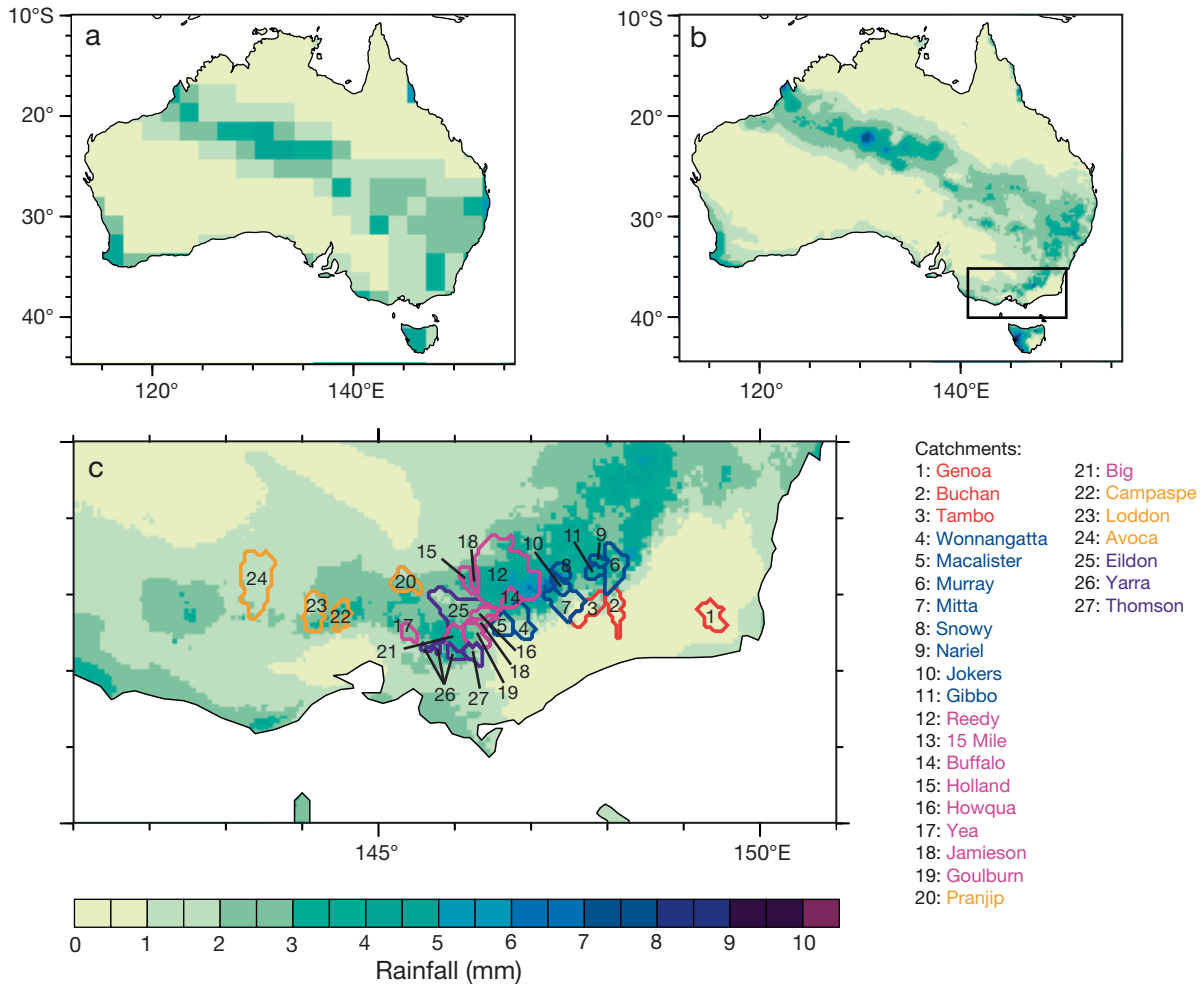

Fig. 1. Schematic of climate model output grid sizes for an example of daily rainfall over Australia shown for (a) a resolution of 1.8° × 1.8° (typical of a climate model), (b) a resolution of 0.05° × 0.05° (achieved using the statistical downscaling method) and (c) the same as (b) but zoomed in on Victoria. Overlaid on (c) are the catchment boundaries, colour coded by region: east (red), alpine (blue), west of Alps (magenta), far west (orange), Melbourne (purple)

11% decline in available surface water has been projected by 2030 (Leblanc et al. 2011).

This study combines 3 existing tools to project streamflow into the future: (1) taking advantage of the information global GCMs can provide about large-scale changes, (2) the statistical downscaling method's ability to translate this into high-resolution rainfall and temperature projections and (3) the simplicity of the streamflow reconstruction method.

2. CATCHMENTS, DATA AND METHODS

2.1 Catchments and observed data

Twenty-seven catchments across Victoria were selected for this study, chosen to represent a diverse range based on yield, location, size and elevation. The catchments were grouped into regions based on their location and streamflow behaviour (Fig. 1). It must be noted that the statewide mean, often referred to in this work for convenience, is the mean of the 27 catchments used here, which do not reflect all catchments within the state; the selected catchments cover about 10% of the state land area and account for about 20% of the total streamflow across the state. Further details and peculiarities of these catchments and regions can be found in Table 1 and Section 2.1 of Fiddes & Timbal (2016).

The streamflow dataset was provided by the Department of Environment, Land, Water and Planning (DELWP) and Melbourne Water to the Bureau of Meteorology (BoM) as a part of the Hydrological Reference Stations dataset (Turner et al. 2012). Catchments within the Hydrological Reference Stations dataset

must meet quality control standards (described at www.bom.gov.au/water/hrs/guidelines.shtml), must have unregulated flows, must have undergone minimal land-use changes and have ≤10% of the flow captured by agricultural use (Sinclair Knight Merz 2010, Turner et al. 2012). Rainfall and temperature data from the Australian BoM's operational high-resolution gridded (0.05° × 0.05°) dataset (Jones et al. 2009) are used. For more information on these datasets, please see the studies referred to and Fiddes & Timbal (2016).

In the present study, anomalies and trends are presented as the percentage of the climatological mean, allowing for simple comparison between catchments. Regional and statewide averages are presented as weighted means of average annual catchment streamflow.

Table 1. CMIP5 climate models used in this study: model name, institution, and spatial resolution in latitude and longitude

Model	Institution name and country	Latitude grid size (km)	Longitude grid size (km)
ACCESS1-0	CSIRO-BoM, Australia	210	130
ACCESS1-.3	CSIRO-BoM, Australia	210	130
bcc-csm1-1-m	BCC, CMA, China	120	120
BNU-ESM	BNU, China	310	310
CanESM2	CCCMA, Canada	310	310
CCSM4	NCAR,USA	130	100
CMCC-CMS	CMCC, Italy	210	210
CNRM-CM5	CNRM-CERFACS, France	155	155
CSIRO-mk3.6	CSIRO-QCCCE, Australia	210	210
GFDL-ESM2G	NOAA, GFDL, USA	275	220
GFDL-ESM2M	NOAA, GFDL, USA	275	220
HadGEM2-CC	MOHC, UK	210	130
IPSL-CM5A-LR	IPSL, France	410	210
IPSL-CM5A-MR	IPSL, France	275	145
IPSL-CM5B-LR	IPSL, France	410	210
MIROC5	JAMSTEC, Japan	155	155
MIROC5-ESM	JAMSTEC, Japan	310	310
MIROC5-ESM-CHEM	JAMSTEC, Japan	310	310
MPI-ESM-LR	MPI-N, Germany	210	210
MPI-ESM-MR	MPI-N, Germany	210	210
MRI-CGCM3	MRI, Japan	120	120

2.2 GCM data

GCM projections developed internationally to underpin the most recent Intergovernmental Panel on Climate Change (IPCC) report (IPCC 2013) and compiled in the CMIP5 database (Taylor et al. 2012) are used in this study. A full list of the 22 models selected, their institution and their horizontal grid size is given in Table 1. Evaluations of model performance in simulating weather and climate phenomena over Australia most pertinent to this study are provided in Table S1 in the Supplement at www.int-res.com/articles/suppl/c071p219_supp.pdf.

Two RCPs have been chosen for this work. RCP 4.5 is characteristic of a stabilization of global anthropogenic emissions and population growth by mid-century and sustainable technological development, resulting in a stable radiative forcing of 4.5 W m^{-2} after 2100 (van Vuuren et al. 2011). RCP 8.5 is that of a continuous increase in global anthropogenic emissions and population and slower development of technology, leading to an unstabilized radiative forcing of 8.5 W m^{-2} by 2100 (van Vuuren et al. 2011).

2.3 Statistical downscaling method

Statistically downscaled GCM output was used to gain higher-resolution (0.05° × 0.05°) rainfall and temperature outputs as illustrated by Fig. 1. The BoM's analogue-based statistical downscaling method (SDM), developed by Timbal & McAvaney (2001), was used to perform the downscaling. Large-scale circulation and weather systems inform local conditions via the search for closely matching daily meteorological analogues based on several synoptic-scale daily predictors. These predictors vary between seasons and across the 3 large climate regions of southeastern Australia. They generally include information about the mean sea-level pressure, large-scale precipitation or specific humidity at 850 hPa, and a horizontal wind component at 850 hPa. Further details of the method and predictors can be found in Timbal et al. (2009).

2.4 Streamflow multiple linear regression

The multiple linear regression, developed by Timbal et al. (2015a) and updated and tested by Fiddes & Timbal (2016), used BoM gridded observations of concurrent and lagged precipitation and the maximum concurrent temperature to reproduce observed monthly streamflow. The Fiddes & Timbal (2016) method, including a longer-term memory, was found to have good skill in capturing the monthly average streamflow, the trends over the 1977–2012 period and the magnitude of the streamflow deficit during

the Millennium drought, except in the driest catchments where it was underestimated. The regression was tested for its ability to reproduce observed streamflow and to ensure that the skill of the model was not artificial via cross-validation, the Nash-Sutcliff efficiency test (Nash & Sutcliffe 1970) and the adjusted explained variance (von Storch & Zwiers 2004). Furthermore, the importance of temperature was tested and found to make little difference to the skill of the model.

Equation (1) describes the regression model (R_1) used throughout this work. R_1 uses the concurrent precipitation and total precipitation of the previous month, previous year and previous 10 yr to compute streamflow, in addition to the concurrent month's maximum temperature. The regressions are applied to each month separately.

$$R_1 = a + bx_1 + cx_2 + dx_3 + ex_4 + fx_5 \quad (1)$$

x_1 = concurrent month's rainfall, x_2 = previous month's rainfall, x_3 = concurrent month's maximum temperature, x_4 = previous 12 month's total rainfall, x_5 = previous 120 month's total rainfall, a to f represent coefficients for each regression.

The effects of including the temperature parameter in the regression were again tested in this study, whereby the temperature coefficient (d) in Eq. (1) is set to zero (denoted throughout work as R_2). Unless specifically stated, results are presented using the full reconstruction (R_1), as the removal of the temperature variable was again found to have little impact on the resulting streamflow prediction.

3. MODEL BIAS CORRECTION AND EVALUATION

3.1 Downscaled CMIP5 precipitation and temperature evaluation

Figure 2 shows the annual cycles of the statistically downscaled CMIP5 models' rainfall and maximum temperatures (over 1950–2005) compared with the observed rainfall and maximum temperature for 4 selected catchments that represent a range of rainfall and streamflow regimes. For rainfall, the models generally underestimate the amount of precipitation across the catchments. On average, the models capture 81% of the observed rainfall mean. The patterns of the annual cycles are generally well represented for rainfall, with the models reproducing the different annual cycle of the eastern catchments (i.e. the Buchan catchment in Fig. 2a). The ensemble's ability to replicate the observed rainfall variance, however, is poor, capturing only 35% of the state's average variance (not shown). While the SDM is successful in removing the large biases found in the direct CMIP5 model simulations of the current climate for large areas (Timbal et al. 2015b), it is clear, even after the statistical downscaling, that further bias correction of the downscaled models is needed to address the remaining issues with both mean and variance.

With regards to maximum temperature, the downscaled models are able to replicate catchment temperature to a high degree. The shape of the annual cycle and the statewide mean are well modelled; however, the variance was overestimated by 28% (not shown).

3.2 Model bias correction

The model evaluation described above suggests that the raw output of the statistically downscaled models needs to undergo some form of bias correction before its application to the streamflow regression. A simple method of 'normalisation' has been applied with respect to observed rainfall and temperature and is described in detail in Part A of the Supplement at www.int-res.com/articles/suppl/c071p219_supp.pdf. This bias correction delivered a much improved representation of rainfall and temperature mean annual cycles across the catchments. For the rainfall, the model variance went from being only 35% of that of the observed data for the same time period to 105% (an overestimation of 5%), and the mean from 81 to 100%. Furthermore, the shape of the annual cycle from the models now matched the observed annual cycle near perfectly. The temperature bias correction saw the variance go from 128 to 105%, whilst the mean and annual cycle continued to be reproduced well.

Applying the streamflow regression after this bias correction showed that the models were now able to reconstruct 104% of the observed mean streamflow, and 99% of the variance. The final stage of removing negative monthly streamflow values (see Part A of the Supplement at www.int-res.com/articles/suppl/c071p219_supp.pdf) and then calibrating against the observations gave the reconstructions a mean of 101% of the observations and variance of 98%. The differences between the reconstructed streamflow using bias-corrected and non-bias-corrected models across all catchments for both mean and variance (Fig. 3) show the significant improvement on a model-by-model basis. However, a residual overestimation of the mean and underestimation of the variance is noted. On

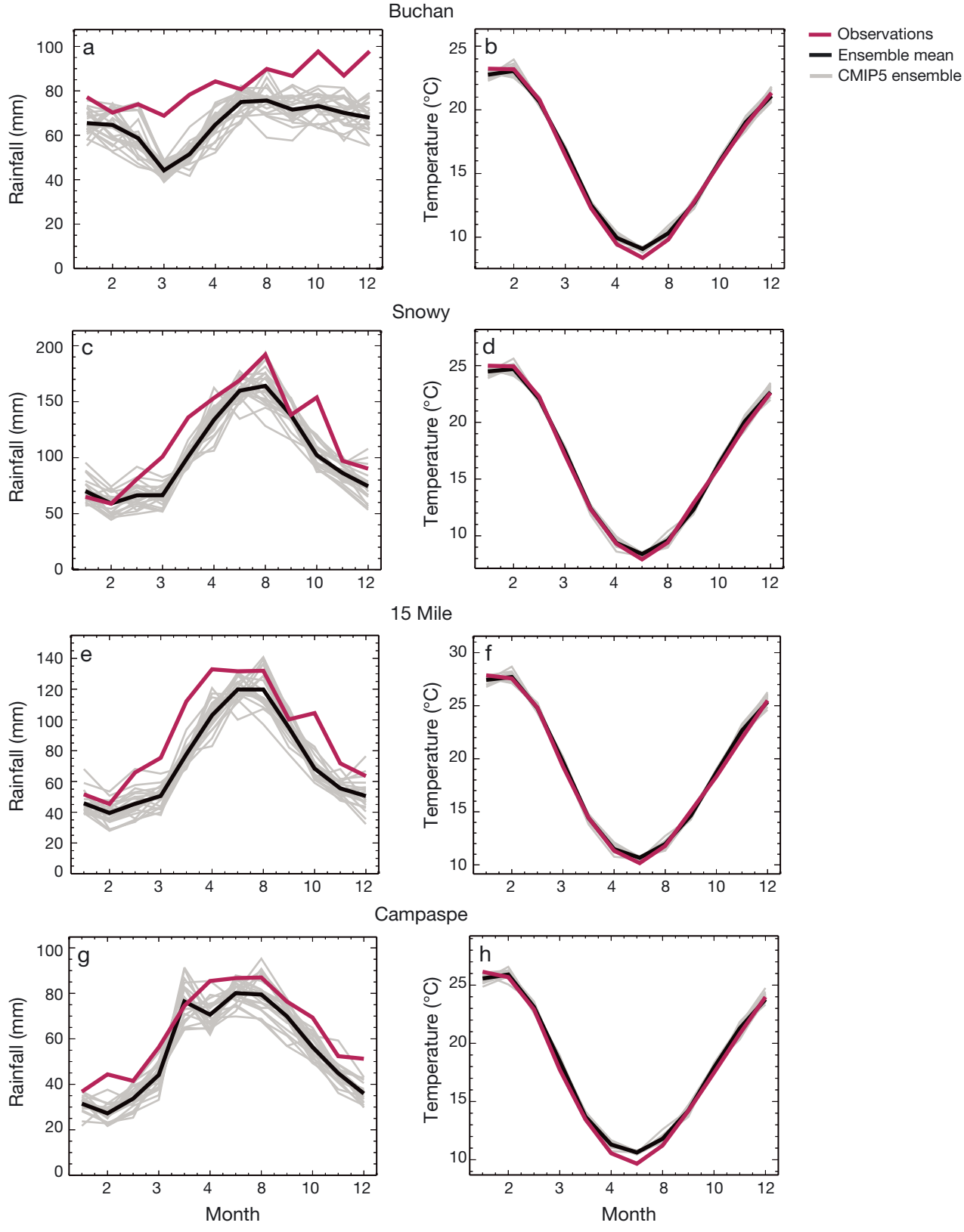

Fig. 2. Annual cycle of rainfall (left) and maximum temperature (right) before bias correction for 4 selected catchments from 4 different sub-regions: (a,b) Buchan from east, (c,d) Snowy from alpine, (e,f) 15 Mile from west of Alps and (g,h) Campaspe from far west. Red: observed rainfall or temperature (BoM gridded observations); black: downscaled model ensemble; grey: individual downscaled models

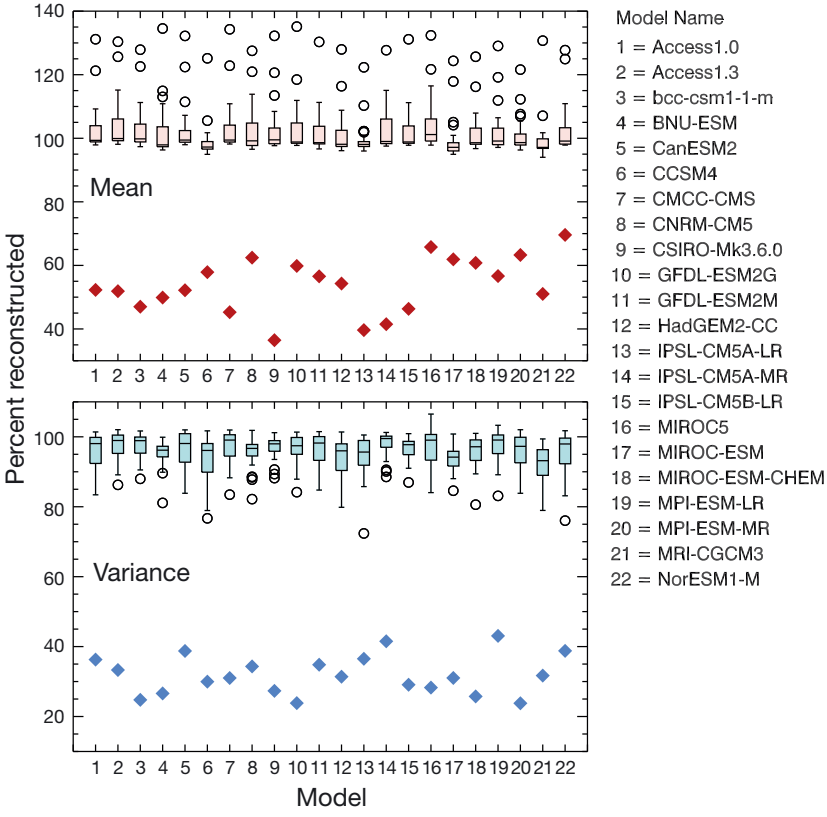

Fig. 3. Percentage of catchment mean (top) and variance (bottom) annual streamflows as reconstructed by R_1 (with temperature) for each downscaled climate model listed on the right. Boxplots: 25th–75th percentile amongst the 27 catchments; horizontal line in box: median; whiskers: maximum or minimum of the data or 1.5 times the 25th or 75th percentile (whichever is smaller); open circles: outliers of the data series; filled diamonds: mean percentage of reconstructed mean (red) or variance (blue) before bias correction was performed

a catchment-by-catchment basis (Fig. 4), it can be seen that spatially, these biases are driven by some catchments that are not well reconstructed by the ensemble mean. This is discussed further in Section 3.3.

Once these methods had been applied to the streamflow data, ranking of the model outputs, based on their reconstruction of the observed streamflow mean and variance, was conducted. These results can be found in Part B of the Supplement at www.int-res.com/articles/suppl/c071p219_supp.pdf. No clear 'best' or 'worst' performing models were found, likely due to the downscaling and bias correction carried out.

3.3 Reconstructed model streamflow across individual catchments

The catchments where the observed mean streamflow from 1975 to 2005 (1977 if observations were not available in 1975) is reproduced most accurately (within 5%) by the ensemble mean are those in the vicinity of the alpine region or just to the west of this (Fig. 4a). Drier catchments are less well reconstructed, in agreement with Chiew et al. (1993) and Fiddes & Timbal (2016). Large bias remains in Avoca in the far west and Genoa in the east (overestimations of 129 and 117%).

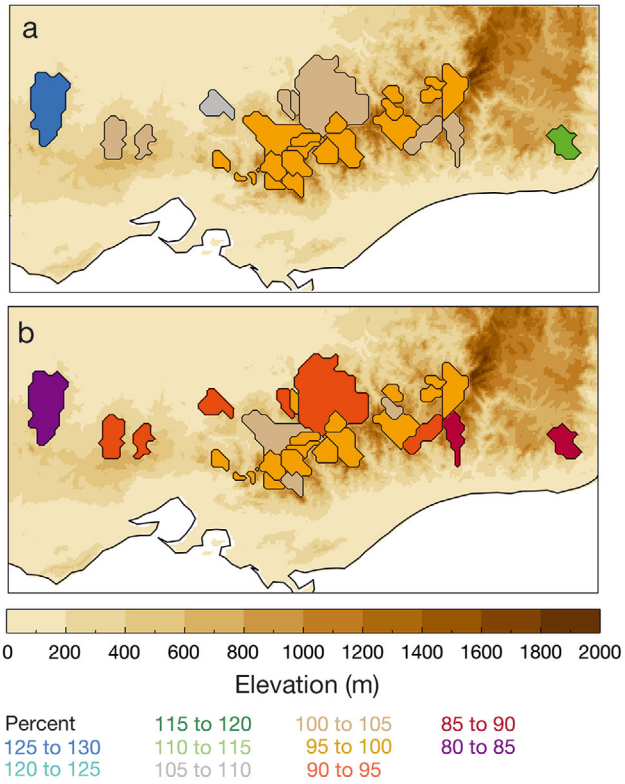

Fig. 4. Reconstructed streamflow (a) mean and (b) variance averaged across the 22 downscaled CMIP5 models for each individual catchment, using R_1. Topography is underlaid

A similar spatial evaluation for the variance (Fig. 4b) shows a large range of results across the catchments. The worst-performing catchments are Avoca in the far west, where only 83% of the variance is captured, and Genoa and Buchan in the east, capturing 88 and 89%.

Modelled historical streamflow time series and annual cycles (Fig. 5) for the 4 representative catchments show that the ensemble mean is generally well matched to the observations. While year-to-year observed and modelled streamflows are not expected to align, the absence of sustained periods of low streamflow similar to the Millennium drought is worth noting. The historical time series from the downscaled Access 1.0 and IPSL-CM5B-LR models have been highlighted to give an idea of individual model's interannual variability; the range of values for annual streamflow is reasonable compared with the observations.

The ensemble mean annual cycle (Fig. 5, right) reconstructs the observations well for most catchments, with the worst performer being the Buchan catchment (Fig. 5b) where the February streamflows are overestimated, likely contributing to the poor performance in general by this catchment's reconstructions. Reconstructions of the other catchments making up the east region do not show this same feature. However, the observed annual cycle of these catchments are unlike other subregions, highlighting the different hydro-meteorological regimes (also seen in Fig. 2a). The fact that the downscaled GCM reconstructions are overall able to capture these differences between catchments highlights the importance of statistical downscaling and its ability to capture finer-scale rainfall regimes. Amongst the 4 selected catchments, the Snowy catchment has the best ensemble mean downscaled GCM reconstruction compared with that of the observations for the annual cycle, and the lowest model spread across the months.

3.4 Historical trends

Climate models generate their own climate interannual and decadal variability; therefore, the GCMs' skill in reproducing the observed climate can only be evaluated from the perspective of the mean and variability, as done above. It is nevertheless of interest to see whether the GCMs are displaying long-term trends through the historical period that resemble what was observed, in particular for the ensemble mean, which can highlight the response to external forcings. Decadal trends for 1977–2012 (Gl decade^{-1}) as a percentage of the 1977–2012 mean show a marked spatial pattern in the observations (Fig. 6a), with sizeable trends, in particular for the drier catchments. The downscaled GCM ensemble means (Fig. 6b) show little trends in general and hardly any spatial contrast between catchments. When individual GCMs are considered, 6 models had statistically significant negative trends in excess of a 5% decline per decade across the state (compared with the observed 7.2% decline), whilst 3 had positive trends in excess of a 5% increase. The remaining 13 GCMs displayed relatively neutral trends. The IPSL-CM5B-LR model provided trends in closest agreement with the observations spatially and in magnitude and sign (Fig. 6c) with an overall decline of 9.4%. These results are in general agreement with results for rainfall in the MDB cluster report, where a large range of rainfall trends across the models was found; with no clear drying trend in the ensemble mean (Timbal et al. 2015b). It should be noted that the majority of the observed trends are not statistically significant at the 90th percentile confidence interval, and individual model results also reflect this, as shown by catchment borders in Fig. 6.

4. FUTURE PROJECTIONS

4.1 Rainfall and temperature projections

Rainfall projections show little difference between RCP 4.5 and RCP 8.5 until mid-century with small mean change from the historical average (Fig. 7a). After mid-century, the 2 emissions pathways separate; RCP 4.5 maintains a constant gradual decline whilst RCP 8.5 displays an increased declining trend. By the end of the century, changes in the cool season from the 1990 mean (1975–2005) for rainfall (Fig. 8a) show, under RCP 4.5, declines of between 5 and 15%, with the catchments in the east region experiencing the greatest declines. RCP 8.5 (Fig. 8b) shows greater declines of approximately 20–30%, and indicates that catchments in the east and far west will experience the biggest cool season changes.

For projected temperature (Fig. 7b), consistent increases extending from the observed period are seen up to 2040, after which the 2 emissions pathways project diverging mean temperatures. Temperatures plateau by 2070 under RCP 4.5, and are increasing at greater rates under RCP 8.5.

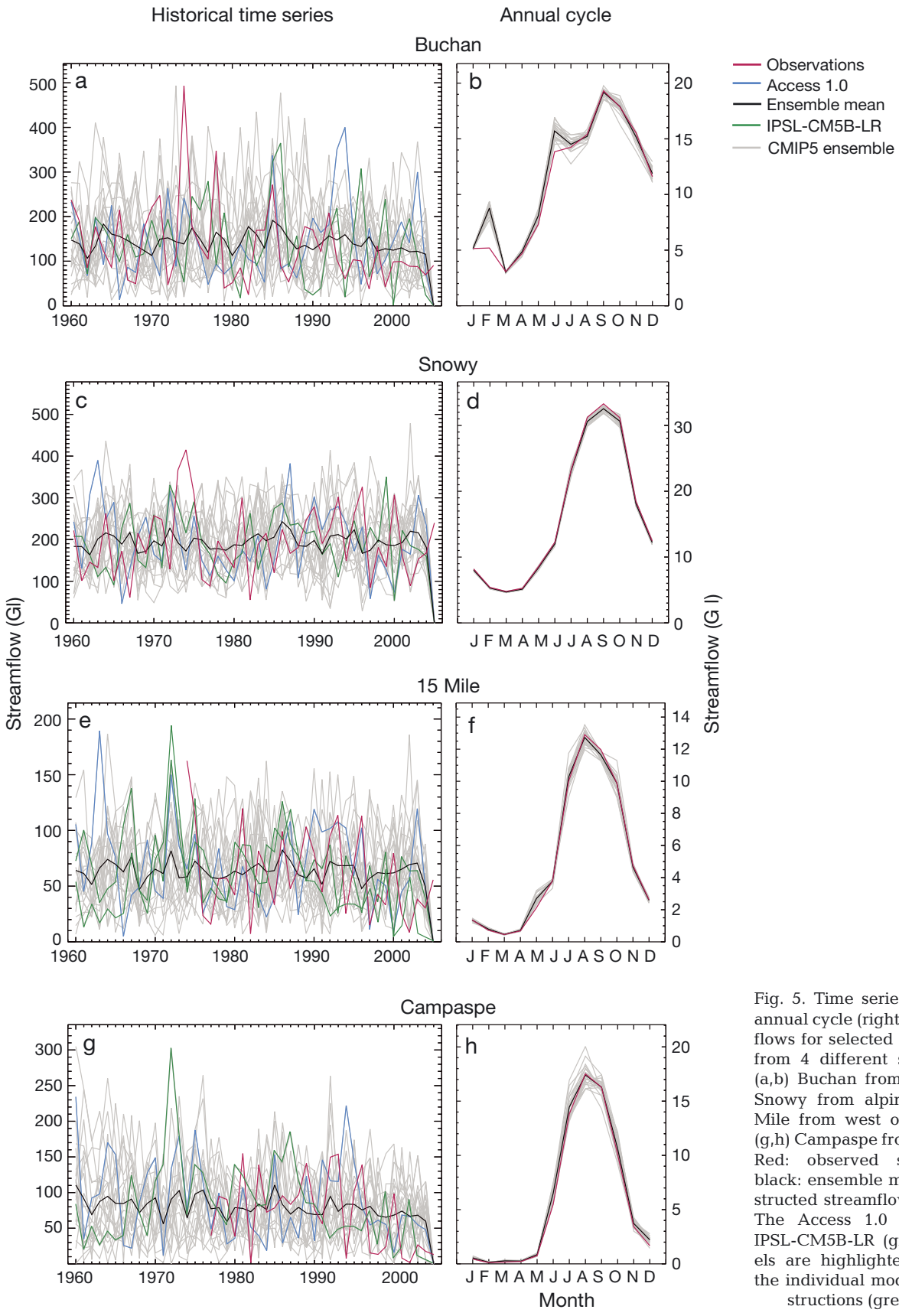

Fig. 5. Time series (left) and annual cycle (right) of streamflows for selected catchments from 4 different subregions: (a,b) Buchan from east, (c,d) Snowy from alpine, (e,f) 15 Mile from west of Alps and (g,h) Campaspe from far west. Red: observed streamflow; black: ensemble mean reconstructed streamflow using R_1. The Access 1.0 (blue) and IPSL-CM5B-LR (green) models are highlighted amongst the individual models' reconstructions (grey lines)

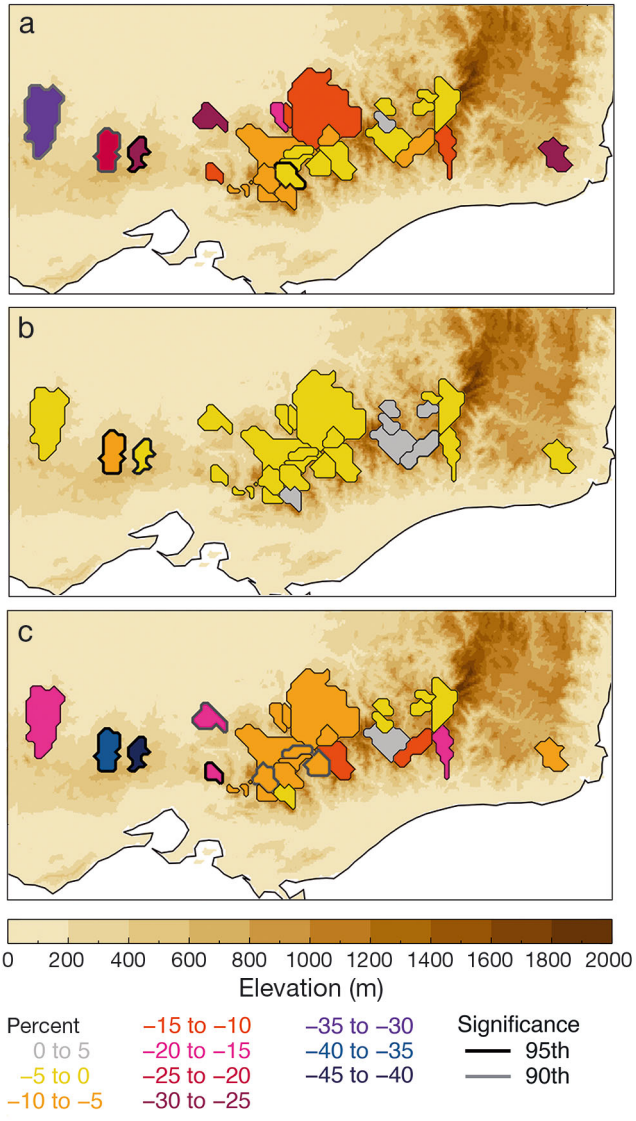

Fig. 6. 1977–2012 linear decadal trends (as a percentage of the period mean) for (a) observed streamflow, (b) the ensemble mean reconstructed streamflow using R_1 and (c) the model (IPSL-CM5B-LR) depicting the most similar trends in the reconstructed streamflow to the observed. Significance at the 90th and 95th percentile confidence intervals are shown by thick grey and thick black boundaries, respectively. Topography is underlaid

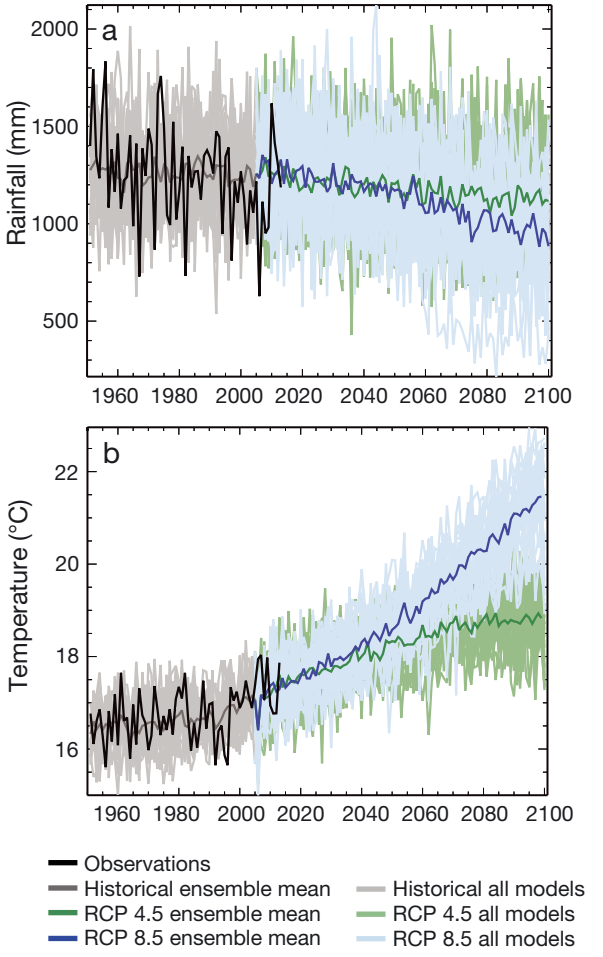

Fig. 7. Time series for Victoria catchment average (a) rainfall and (b) temperature for 1950 to 2010 as simulated by the statistical downscaling of the CMIP5 models. Black: observed time series from 1950 to 2013; dark lines: model ensemble means; lighter lines: individual model projections; grey: historical period (1960–2005); the future period (2005–2100) — green: RCP 4.5, blue: RCP 8.5

4.2 Future streamflow estimates

From these changes in rainfall and temperature, the time series of projected streamflow for both emissions pathways were computed for the average of the 27 Victoria catchments and their respective regions (Fig. 9). In these plots, the average of the historical observed mean, the mean streamflow experienced during the Millennium drought and the 2070–2100 projected ensemble means and model mean range (error bars) for both emissions pathways and both regression methods are compared (right box in each panel). The range of model outputs remains relatively constant over the entire period, as does the interannual variability. The 2 projected time series, RCP 4.5 (green) and RCP 8.5 (blue), are similar in decline until mid-century (1–37 and 7–36% 2035–2065 declines from the historical mean, respectively), after which they begin to separate, as per the rainfall projections.

The overall 2070–2100 projected streamflow average for the 27 catchments following RCP 4.5 is 26% (5–41% uncertainty range) less than the historical mean (Table 2). Under RCP 8.5 the 2070–2100 average projected streamflow is 45% (24–87%) less than

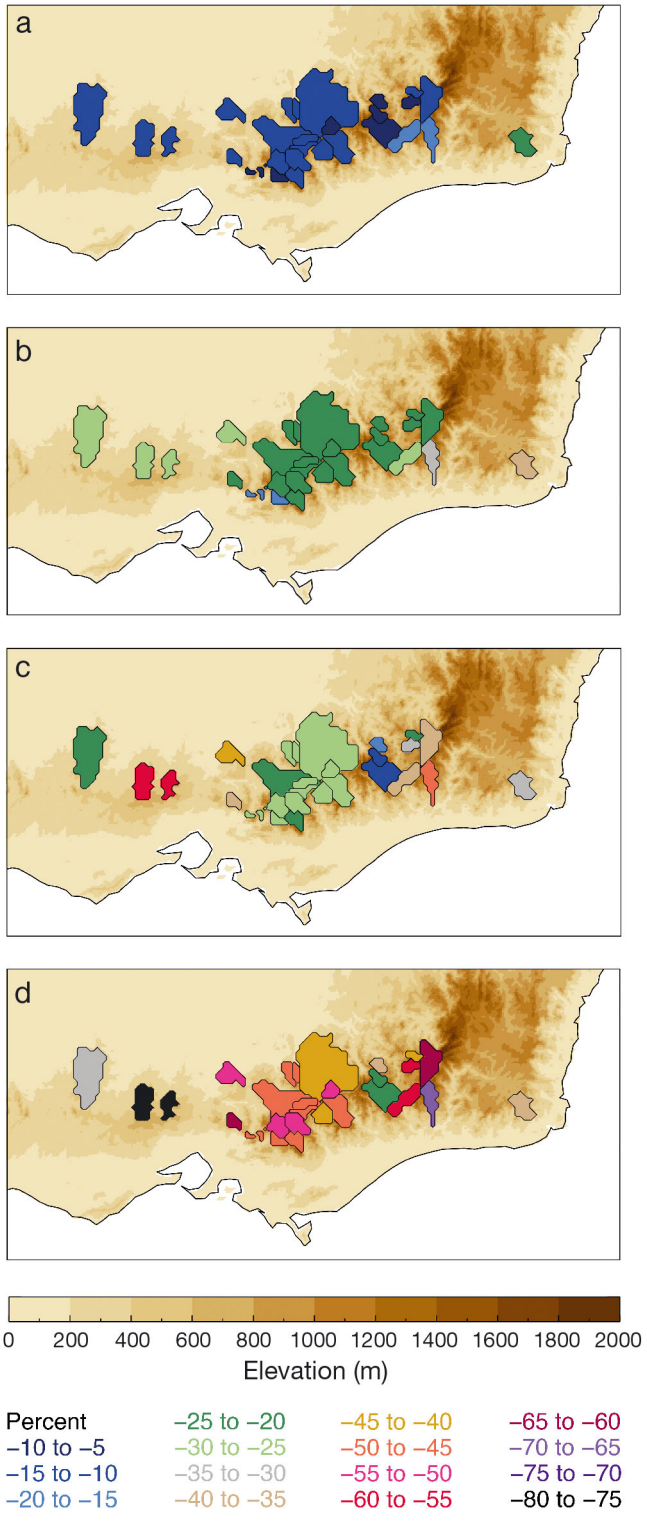

Fig. 8. Mean cool season (April to October for rainfall and May to November for streamflow) change in (a,b) rainfall and (c,d) streamflow using R_1 for the 2070–2100 period (in percent change from the 1975–2005 reconstructed mean) following (a,c) RCP4.5 and (b,d) RCP 8.5 emissions pathways. Topography is underlaid

the historical mean, which is greater than the decline experienced during the Millennium drought (31.3%). Figure 8c,d provides a spatial perspective of these trends, outlining the dependence of the magnitude of the cool season decline on the position of the catchment relative to the Alps, a pattern reminiscent to what has been observed for recent observed trends (Fig. 6a).

By region, catchments in the east and far west, which experienced the largest deficits during the Millennium drought (Fiddes & Timbal 2016), appear to experience the largest declines by the end of the century, under RCP 8.5 (Table 2), despite some of these catchment reconstructions overestimating observed streamflows. Avoca and Genoa were shown earlier to have the largest overestimations (129% and 117%) in the bias-correction phase, implying that these changes in mean could be much greater than what is calculated here. Looking at other catchments in the east and far west regions, the Buchan, Loddon and Campaspe catchments report annual declines from 1990 of 56% (25–84%), 74% (50–96%) and 76% (48–95), respectively. These results are in agreement with current trends, respectively and are again larger deficits than those experienced annually during the Millennium drought (55, 66 and 72% of the observed mean).

Across the other catchments, although lesser declines are experienced compared with the east and far west, they are generally between 1.0 and 2.5 times greater than the respective deficit that was experienced during the Millennium drought.

The impact of including temperature in the statistical reconstruction of streamflows across the 27 catchments (Fig. 9 and Table 2) appears very small overall. An analysis of the top and bottom 5 performing models streamflow projections is presented in Table S2 of Supplement B at www.int-res.com/articles/suppl/c071p219_supp.pdf.

4.3 Annual cycle changes

The annual cycles of projected streamflows are investigated (Fig. 10) and summarised for cool and warm season averages (Table 2). The average RCP 8.5 streamflow response across the 27 catchments (Fig. 10a) shows little changes during the warm season relative to the historical modelled streamflows (grey) and the GCM model spread is also largely unchanged, for both periods of time. In percentage terms, the change between the 1975–2005 downscaled GCM mean and the RCP 8.5 2035–2065 and

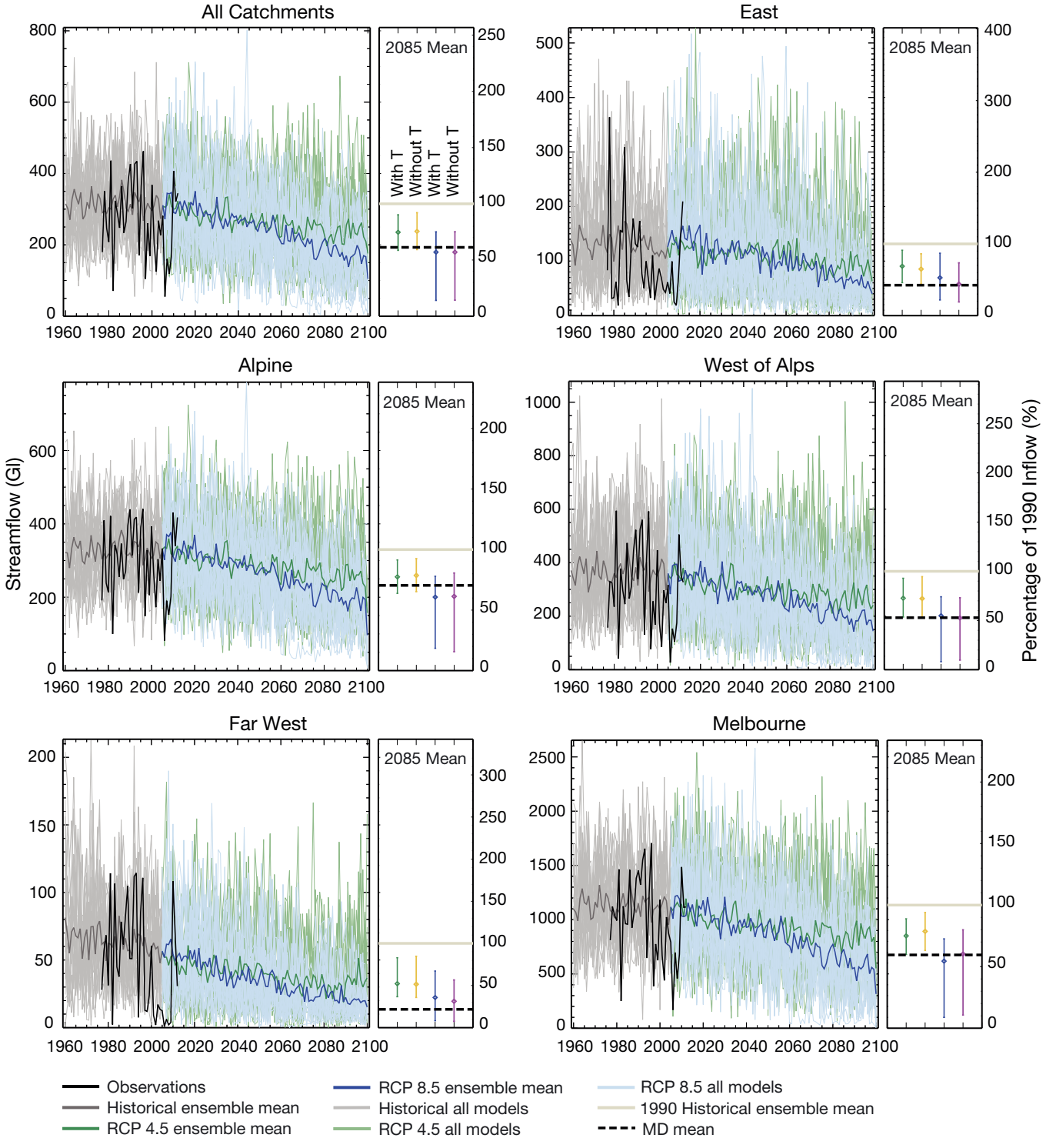

Fig. 9.(Top left) Annual streamflow time series average across the 27 catchments in Victoria from 1960 to 2100. Black: observed streamflow from the Bureau of Meteorology Hydrological Reference Stations. Grey: modelled streamflows for the historical period (1960 to 2005s) and for 2006 to 2100 using RCP 4.5 (green) and RCP 8.5 (blue). Lighter lines: individual models, thick lines: ensemble means. Chart on the right: diamonds show the 2070–2100 ensemble mean for both RCP 4.5 and RCP 8.5 and using a streamflow reconstruction with (R1; green and blue) and without (R2; yellow and purple) concurrent maximum temperature; error bars display the maximum and minimum 2070–2100 individual model means. Also shown: the 1975 to 2005 mean (light grey line) and the observed deficit during the Millennium drought (1997–2009, dashed black line). This is repeated for the subregions east, alpine, west of Alps, far west and Melbourne

Table 2. Downscaled climate models mean changes for annual, cool (May–November) and warm (December–April) seasonal streamflows. Changes are provided for the 2035–2065 (2050) and 2070–2100 (2085) periods, shown as a percent change from the reconstructed 1975–2005 (1990) reference period, following RCP 4.5 and RCP 8.5 and using 2 statistical reconstructions with (R_1) and without (R_2, in brackets) monthly temperature

Catchment	Annual		Cool season		Warm season	
	RCP 4.5	RCP 8.5	RCP 4.5	RCP 8.5	RCP 4.5	RCP 8.5
2050						
East	−12.3 (−16.0)	−18.0 (−22.7)	−17.7 (−21.6)	−24.8 (−29.9)	5.7 (3.5)	5.1 (2.1)
Alpine	−12.9 (−11.5)	−17.1 (−15.5)	−14.1 (−12.9)	−18.7 (−17.2)	−7.0 (−4.8)	−9.6 (−7.1)
West of Alps	−18.5 (−17.2)	−23.9 (−22.7)	−19.6 (−18.2)	−25.1 (−23.7)	−4.8 (−5.6)	−9.8 (−10.5)
Far west	−31.0 (−32.9)	−40.6 (−43.7)	−32.2 (−34.2)	−41.7 (−45.0)	−12.0 (−12.8)	−21.0 (−21.8)
Melbourne	−16.0 (−12.8)	−21.4 (−17.3)	−16.9 (−13.6)	−22.5 (−18.2)	−9.0 (−6.5)	−13.1 (−10.4)
Average	−16.2 (−15.0)	−21.4 (−20.1)	−17.7 (−16.5)	−23.1 (−21.8)	−5.9 (−5.3)	−9.8 (−9.0)
2085						
East	−31.6 (−35.5)	−48.4 (−56.9)	−38.6 (−42.7)	−55.3 (−64.5)	−7.9 (−10.7)	−25.0 (−30.3)
Alpine	−21.9 (−20.3)	−38.9 (−37.8)	−23.3 (−21.8)	−41.8 (−41.0)	−15.2 (−13.5)	−25.1 (−22.7)
West of Alps	−27.5 (−26.3)	−47.2 (−46.3)	−28.5 (−27.2)	−49.2 (−48.2)	−14.3 (−15.1)	−21.6 (−22.9)
Far west	−41.8 (−45.6)	−56.7 (−66.5)	−42.8 (−46.9)	−58.6 (−69.2)	−21.6 (−22.6)	−24.1 (−25.5)
Melbourne	−24.8 (−20.7)	−46.0 (−39.3)	−25.5 (−21.1)	−47.8 (−40.6)	−19.3 (−17.0)	−32.0 (−29.2)
Average	−26.1 (−24.8)	−44.8 (−44.0)	−27.6 (−26.3)	−47.5 (−46.7)	−15.6 (−15.1)	−25.1 (−24.7)

2070–2100 downscaled GCM mean for the warm season is −10% and −25%, respectively (Table 2). Once again, little difference in streamflow deficits is found when temperature is removed from the reconstructions.

For the cool season (May to November), the changes relative to the 1975–2005 mean are larger, in particular for 2085 (2070–2100). The 2035–2065 mean change (red) from 1975–2005 is −23% and for 2070–2100 (orange) is −47% under RCP 8.5. The range of model results for both time periods is larger during the cool season (compared with the 1975–2005 in grey), implying less model agreement. The shape of the catchment average annual cycle remains relatively constant across the 3 time periods, where August continues to be the month of maximum streamflow, with no shift of seasonality. Regional changes in monthly streamflow follow trends that are largely reflected in the 27 catchment average. However, some peculiar results are obtained for certain months in certain regions.

In the east region, where models are consistently overestimating observed streamflow, an increase in streamflow of 5% during the warm season for the 2035–2065 (RCP 8.5) mean is seen, reversing to a mean decline of 25% by 2070–2100 (Table 2). For the cool season, declines in the mean are 25 and 55% by 2035–2065 and 2070–2100, respectively, with the caveat of the lower skill in the east region, particularly for Genoa. With this in mind, some features of this projection have to be considered with circumspection, such as the large peaks in June (where there is also large inconsistency between models) found in the reconstructions but not the observations. When only the top 5 models for the east region (not shown) are considered, some of these spurious behaviours are reduced but not necessarily eliminated.

For the far-west catchments (Fig. 10e), the peak of the streamflow appears to shift from August to October by the end of the century, and appears to increase. Exploration of the top 5 models (not shown) indicates that this result is not due to one model but is a feature of the best-performing models, where strong agreement is seen, therefore increasing the confidence in this result. Despite this, however, the overall cool season decline is 42% by 2050 and 59% by 2085.

4.4 Long-term drought risk

As future projections consistently point towards a reduction of streamflow, the frequency of years in which average streamflow is below that experienced during the Millennium drought (a deficit of 31.3%) has been evaluated for the first and second halves of the 21st century (Table 3). In the 2005–2050 period, the 2 emissions pathways show a very similar number of years; the model ensemble mean giving 14 and 16 for RCP 4.5 and RCP 8.5, respectively. This result is proportionally larger than the historical reconstructions (11 out of 46 years) and the observed streamflow (7 out of 31 years). For the second half of

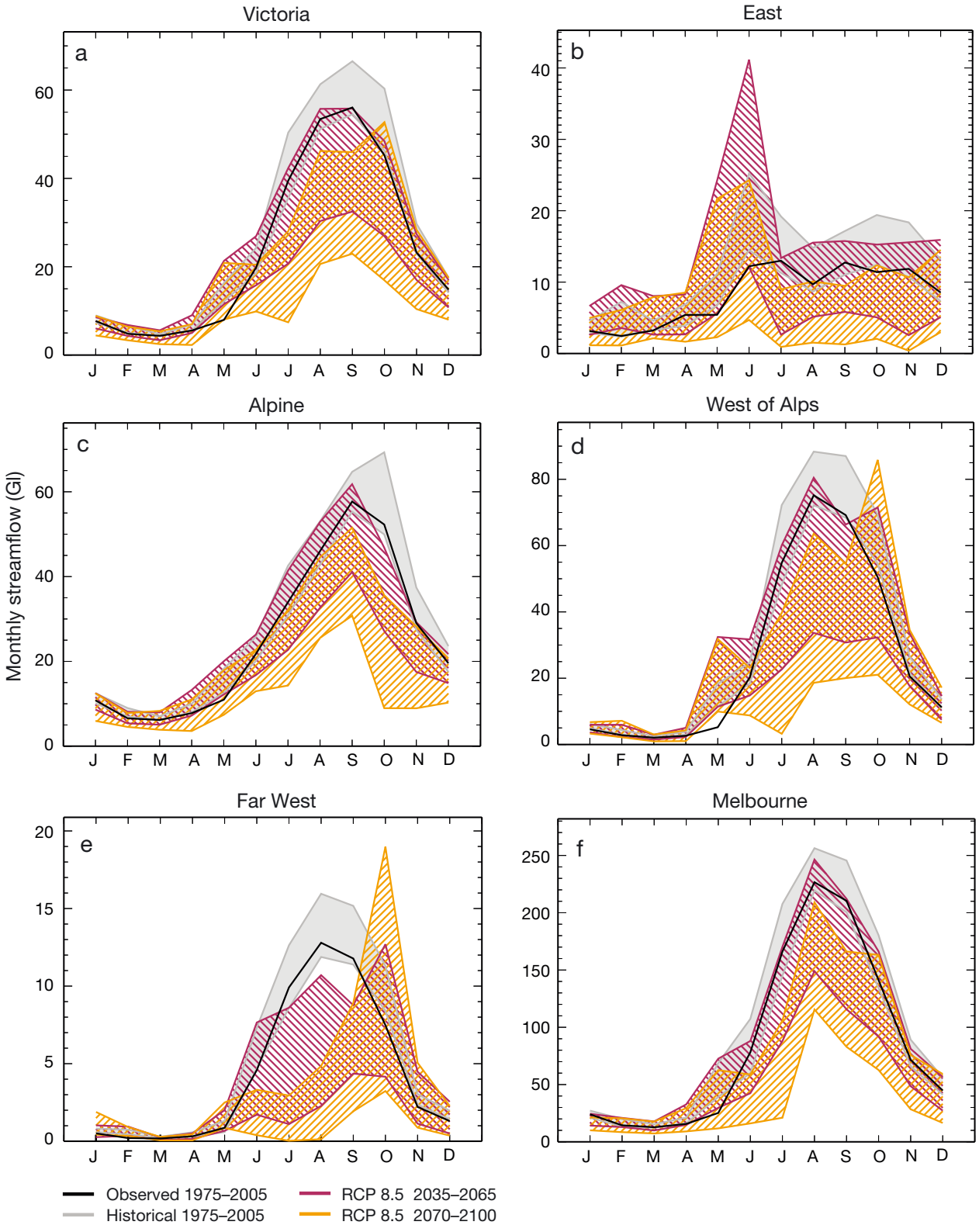

Fig. 10. Range of results for all models reconstructing the annual streamflow cycle (Gl), using R_1, under RCP 8.5 for (a) Victoria. The observed 1975–2005 mean streamflow is plotted in black along with the range of model results for: historical 1990 (1975–2005) mean (grey solid), 2050 (2035–2065) mean (red striped) and 2085 (2070–2100) mean (orange striped). (b–f): the same as (a) but for the subregions (b) east, (c) alpine, (d) west of Alps, (e) far west and (f) Melbourne

Table 3. Number of years where the annual 27 catchment average streamflow deficit (in percent of model reconstructed historical mean) is below the mean deficit observed during the Millennium drought (MD, in percent of observed mean) for the first and second half of the 21st century, using RCP 8.5 and RCP 4.5 and the R_1 reconstruction (with temperature). Rightmost 2 columns: lowest 10 yr mean streamflow expected between 2051–2100 as a percentage of the reconstructed historical mean; values below what was experienced during the MD (–31.3%) are in **bold**. Results are shown for the 22 CMIP5 downscaled climate models individually with the ensemble mean in the last row

	No. of years below MD average				Driest 10 yr period	
	2005–2050		2051–2100		2051–2100 (%)	
	RCP 4.5	RCP 8.5	RCP 4.5	RCP 8.5	RCP 4.5	RCP 8.5
Access1.0	14	16	21	30	**–36.2**	**–60.4**
Access1.3	21	9	25	38	**–42.2**	**–70.5**
bcc-csm1-1-m	11	22	26	31	**–48.1**	**–54.9**
BNU-ESM	23	10	33	46	**–57.7**	**–89.5**
CanESM2	10	17	27	27	**–46.1**	**–42.3**
CCSM4	14	10	18	22	–30.9	**–54.8**
CMCC-CMS	11	12	30	34	**–51.5**	**–65.0**
CNRM-CM5	12	11	29	31	**–51.9**	**–59.4**
CSIRO-Mk3.6.0	11	12	14	22	–30.1	**–43.3**
GFDL-ESM2G	8	10	27	27	**–50.2**	**–64.2**
GFDL-ESM2M	9	13	20	34	**–38.3**	**–61.5**
HadGEM2-CC	16	13	24	30	**–50.6**	**–59.2**
IPSL-CM5A-LR	13	11	17	33	**–39.4**	**–58.4**
IPSL-CM5A-MR	11	11	23	30	**–40.1**	**–71.7**
IPSL-CM5B-LR	8	14	21	22	**–45.1**	**–46.1**
MIROC5	17	20	20	22	**–34.5**	**–43.1**
MIROC-ESM	10	12	16	24	**–33.7**	**–41.8**
MIROC-ESM-CHEM	8	9	14	27	–25.6	**–48.7**
MPI-ESM-LR	11	10	22	31	**–46.2**	**–50.1**
MPI-ESM-MR	14	17	18	28	**–45.8**	**–66.3**
MRI-CGCM3	11	13	12	22	–23.1	**–37.5**
NorESM1-M	15	18	31	26	**–48.3**	**–43.1**
Ensemble mean	13	13	22	29	**–41.6**	**–56.0**

the century (2051–2100), it is estimated that 21 of the 50 years will be below that threshold, assuming the RCP 4.5 pathway, rising to 30 for RCP 8.5.

Table 3 additionally shows what to expect for the driest 10 yr period in the second half of the 21st century. Such periods are projected to be 32% worse than the Millennium drought (41% instead of 31%) following RCP4.5 and 78% worse than the Millennium drought with RCP8.5 (56% instead of 31%).

Another way to look at drought risk over a number of years is using a drought depth duration (DDD) curve (Timbal & Fawcett 2013). DDD curves (Fig. 11) show the magnitude of the driest n-yr average, from 1 yr up to 31 yr, for the first and second half of the century, as a percentage of the reconstructed 1960–2005 mean, for the 2 emissions pathways. The curves for the observed streamflow (as a percentage of the 1975–2005 mean) and reconstructed streamflow for the historical period (1960–2005) are shown as reference for all future periods.

For the historical reconstruction, the driest 1 yr is shown to be a 63% reduction from the 1960–2005 mean and for the observed climate (black) the driest 1 yr period was a 79% reduction (from the 1975–2005 mean). As we progress along the *x* axis (longer period), the driest n-yr period declines in magnitude, until at the 31 yr period, both the observed and historical reconstructed streamflow are under 4%, implying that the driest 31 yr period is close to the mean, as expected since the record is relatively short. It is worth noting that the shape of the observed DDD curve is not well matched by the model reconstruction for the historical period. Mid-length durations up to 18 yr are more severe in the observed world, which reflects the fact that no climate model simulated a drought of similar magnitude or duration as the Millennium drought.

For future projections, RCP 4.5 and RCP 8.5 over 2005–2050 (Fig. 11a,b), the severity of the driest 1 yr increased relative to the reconstructed historical climate, but remained less than observed. The shape of the DDD curve for both RCPs is similar to, although separated from, the historical climate, indicating that we are seeing a shift in the base climate rather than increased severity for periods of particular duration.

In the second half of the century, an increase in magnitude for all the driest n-yr periods over the 2051–2100 period is obvious (Fig. 11c,d). For RCP 4.5, at the 1–5-yr scale, a deficit of magnitudes similar to that experienced in the observed climate are noted; however, for RCP 8.5 we are seeing greater deficits at even the shorter time periods. The driest 31 yr periods are now approximately 28 and 44% drier than that of the reconstructed and historical climate for each RCP pathway, respectively, matching the mean declines discussed in Section 4.2.

5. DISCUSSION AND CONCLUSION

In this study, streamflows for 27 of Victoria's water catchments were projected to the end of the 21st

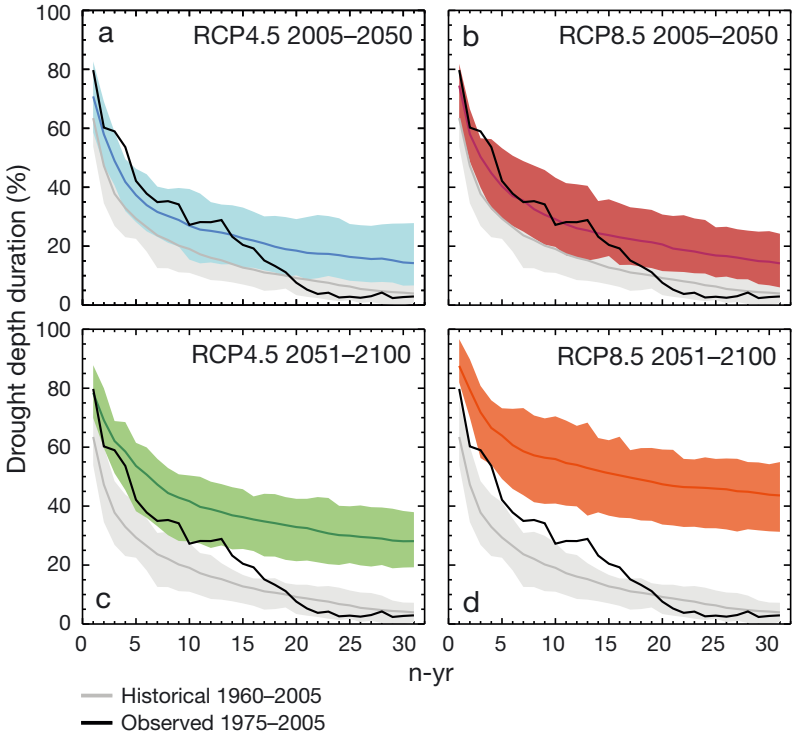

Fig. 11. Streamflow drought depth duration, using R_1 — solid coloured lines: ensemble means for the driest n-yr mean within a 31 yr period for the periods (a,b) 2005–2050 and (c,d) 2051–2100 for (a,c) RCP4.5 and (b,d) RCP 8.5. Grey line: ensemble mean reconstructed historical average (1960–2005) for any n-yr period. Shaded bands: 10th and 90th percentiles for the model ensemble. Black lines: observed historical average (1975–2005)

century using 22 statistically downscaled CMIP5 GCMs and a multiple linear regression on rainfall and temperature parameters to compute monthly streamflows. Initial assessment found the models needed bias correction with respect to the observed rainfall, temperature and streamflow data before the historical streamflow could be reconstructed satisfactorily. An average of 101% of the observed mean and 98% of the variance was captured after this step.

Results across all catchments indicate that by 2050 under RCP 8.5 (RCP 4.5), streamflow will be 21% (16%) less than the 1990 average. By 2085 this increases to 45% (26%). Under RCP 8.5, streamflow declines are expected to be greater in magnitude than what was experienced during the Millennium drought (a 31.3% decline of observed mean).

The biggest declines are expected in the cool season (May–November), with little shift in the annual cycle expected. The likelihood of years with streamflows less than that experienced during the Millennium drought is to increase to just under half of all years in the 2051–2100 period under RCP 4.5 and over half under RCP 8.5. A shift towards more frequent dry years will give catchments less opportunity to recuperate in the average or wetter years, putting them under increasing stress (Saft et al. 2015). The driest 10 yr period in the 2051–2100 period is projected to be 32% worse than the Millennium drought following RCP4.5 and up to 78% worse than the Millennium drought with RCP8.5.

Overall, these results do not depart significantly from previous studies using rainfall–runoff hydrological models (Leblanc et al. 2011, CSIRO 2012, Post & Moran 2013) while confirming spatial differences observed during extended periods of reduced rainfall such as the Millennium drought. While it has been shown that the multiple linear regression produces extreme drought conditions in the future, these events may be more severe than presented here due to its reliance on a linear method (Sachindra et al. 2013).

Historical observations suggest that the catchments that will experience the largest declines in streamflow will be those that currently receive the least rainfall in the far west and east of the state (Fiddes & Timbal et al. 2016). While 2 of these catchments are poorly reconstructed and remain uncertain (Avoca and Genoa), projections for the remaining catchments in these regions confirm this with much larger declines in annual streamflow, of as much as 76% for the Campaspe catchment. Wetter catchments near the mountains, whilst not projected to experience such large declines, will still experience streamflow deficits worse than what they experienced during the Millennium drought in terms of both streamflow and rainfall. One caveat of this work is the assumption that the relationship of rainfall and temperature to streamflows will remain linear throughout the 21st century. Whilst we have no way of determining otherwise, by knowing that the response of streamflow to the climate is non-stationary (Saft et al. 2015, Fiddes & Timbal 2016), these results must be used with caution. Nevertheless, at the monthly timescale, previous studies have suggested that the use of multiple linear regression is appropriate to compute streamflows (Chiew 1993, Sachindra et al. 2013), and the historical reconstructions presented here are of satisfactory skill. Our

knowledge of how catchments behave under stress and the limitation of the multiple linear regression implies that the effects of rainfall reduction and warming temperatures could be larger than what is captured in this work, especially in the worst-affected catchments.

Further uncertainties lie inherently with the use of GCMs, and their respective emissions pathways, especially in their low skill in reproducing historical trends in precipitation (and subsequently streamflow). One reason for this will be due to the GCMs' internally generated climate not experiencing a Millennium drought at the end of the period, whilst systematic biases, not able to be rectified by the statistical downscaling and bias-correction phases, are also responsible.

Arguments exist as to the appropriateness of GCM rainfall projections in hydrological impact studies. Despite the uncertainties discussed above, we believe these remain the best tool available to gain some insight into the changes in future climate. We note that it is not the absolute rainfall or streamflow projections that are important in studies such as these, rather the change from each model's internal historical mean.

Additionally, we are given greater confidence in the rainfall projections when looking at studies exploring southeastern Australian rainfall trends in connection with climate drivers such as the Sub-Tropical Ridge, the El Niño/Southern Oscillation, the Indian Ocean Dipole or the Southern Annular Mode. Such work implies that with future warming, and subsequent changes in the large-scale circulation of the atmosphere, precipitation will decrease (Weller & Cai 2013, Hendon et al. 2014, Grose et al. 2015b, Lim et al. 2016). This is in agreement with the ensemble mean rainfall trend found in this study. With greater confidence in GCM projections of large-scale phenomena, the use of these statistically downscaled GCMs in this work is further justified, and can provide important information, especially with respect to changes over time.

Results from this study indicate that whilst catchments across Victoria will respond differently to the effects of climate change, the majority are projected to see reductions in streamflow of greater magnitude than those experienced during the Millennium drought by the end of the century, severely limiting Victoria's water capacity if it were to rely on rainfall alone. Alternative water sources, along with more efficient water management and use, will be essential in the future if the state is to provide for increasing population demands.

Acknowledgements. Streamflow data for this study were provided by G. Amirthanathan (Bureau of Meteorology) and the downscaled climate projection data were prepared by J. Siddaway. We thank K. S. Tan and Rae Moran for their comments on this work. We acknowledge the World Climate Research Programme's Working Group on Coupled Modelling, which is responsible for CMIP, and we thank the climate modelling groups (listed in Table 1) for producing and making available their model output. Thanks also to Alexandre Pezza (University of Melbourne) for his support of S.F. as part of the ARC (Grant no. DP120103950). B.T.'s contribution to this work was supported by the Victorian Climate Initiative (VicCI).

LITERATURE CITED

Chiew FHS (2006) Estimation of rainfall elasticity of streamflow in Australia. Hydrol Sci J 51:613–625

Chiew FHS, Stewardson MJ, McMahon TA (1993) Comparison of six rainfall-runoff modelling approaches. J Hydrol 147:1–36

Chiew FHS, Vaze J, Viney NR, Perraud JM, Teng J, Post DA (2008) Modelling runoff and climate change impact on runoff in 178 catchments in the Murray–Darling Basin using Sacramento and SIMHYD rainfall-runoff models. In: Lambert M, Daniell, TM, Leonard, M (eds) Proc Water Down Under 2008, Engineers Australia, Barton, p 87–97

CSIRO (2010) Climate variability and change in south-eastern Australia: a synthesis of findings from Phase 1 of the South Eastern Australian Climate Initiative (SEACI). CSIRO, Canberra. www.seaci.org

CSIRO (2012) Climate and water availability in southeastern Australia: a synthesis of findings from Phase 2 of the South Eastern Australian Climate Initiative (SEACI). CSIRO, Canberra. www.seaci.org

CSIRO, BoM (Bureau of Meteorology) (2015) Climate change in Australia information for Australia's natural resource management regions: technical report. CSIRO and Bureau of Meteorology. www.climatechangeinaustralia.gov.au/

DTPLI (Department of Environment, Land, Water and Planning) (2014) Victoria in future 2014: populations and household projections to 2051. Demographic and Spatial Research, Department of Transport, Planning and Local Infrastructure, Melbourne. www.dtpli.vic.gov.au/victoria-in-future-2014

Fiddes SL, Timbal B (2016) Assessment and reconstruction of catchment streamflow trends and variability in response to rainfall across Victoria, Australia. Clim Res 67:43–60

Grose M, Abbs D, Bhend J, Chiew F (2015a) Southern slopes cluster report. In: Ekstrom M, Whetton P, Gerbing C, Grose M and others (eds) Climate change in Australia projections for Australia's natural resource management regions: cluster reports. CSIRO and Bureau of Meteorology

Grose M, Timbal B, Wilson L, Bathols J, Kent D (2015b) The subtropical ridge in CMIP5 models, and implications for projections of rainfall in southeast Australia. Aust Meteorol Oceanogr J 65:90–106

Hendon HH, Lim EP, Nguyen H (2014) Seasonal variations of subtropical precipitation associated with the Southern Annular Mode. J Clim 27:3446–3460

IPCC (Intergovernmental Panel on Climate Change) (2007)

Climate change 2007: synthesis report. Contribution of Working Groups I, II and III to the Fourth Assessment Report of the Intergovernmental Panel on Climate Change. IPCC, Geneva

IPCC (Intergovernmental Panel on Climate Change) (2013) Climate change 2013: the physical science basis. Contribution of Working Group I to the Fifth Assessment Report of the Intergovernmental Panel on Climate Change. IPCC, Geneva

Irving DB, Whetton P, Moise AF (2012) Climate projections for Australia: a first glance at CMIP5. Austr Met and Oceon Jour 62:211–225

Jones DA, Wang W, Fawcett R (2009) High quality spatial climate data sets for Australia. Aust Met Ocean J 58:233–248

Leblanc M, Tweed S, Van Dijk A, Timbal B (2011) A review of historic and future hydrological changes in the Murray–Darling Basin. Global Planet Change 80–81: 226–246

Lim EP, Hendon HH, Arblaster JM, Delage F, Nguyen H, Min SK, Wheeler MC (2016) The impact of the Southern Annular Mode on future changes in Southern Hemisphere rainfall. Geophys Res Lett 43:7160–7167

Murphy RE, Moran R, Hill PI, Jusuf K (2010) Quantifying the post-1997 climate shift in Victoria. In: Climate change 2010: practical responses to climate change. Engineers Australia, Barton, p 237–251

Nash JE, Sutcliffe JV (1970) River flow forecasting though conceptual models. 1. A discussion of principles. J Hydrol (Amst) 10:282–290

Post DA, Moran RJ (2013) Provision of usable projections of future water availability for southeastern Australia: the South Eastern Australian Climate Initiative. Aust J Water Resour 17.2:135–142

Potter NJ, Chiew FHS (2009) Statistical characterisation and attribution of recent rainfall and runoff in the Murray–Darling Basin. In: Anderssen RS, Braddock RD, Newham LTH (eds) 18th World IMACS Congress and MODSIM09 International Congress on Modelling and Simulation. Modelling and Simulation Society of Australia and New Zealand and International Association for Mathematics and Computers in Simulation, July 2009, p 2812–2818. www.mssanz.org.au/modsim09/F12/kragt.pdf

Sachindra DA, Huang F, Barton A, Perera BJC (2013) Least square support vector and multi-linear regression for statistically downscaling general circulation model outputs to catchment streamflows. Int J Climatol 33:1087–1106

Sachindra DA, Huang F, Barton A, Perera BJC (2015) Potential improvements to statistical downscaling of general circulation model outputs to catchment streamflows with downscaled precipitation and evaporation. Theor Appl Climatol 122:159–179

Saft M, Western AW, Zhang L, Peel MJ, Potter NJ (2015) The influence of multiyear drought on the annual rainfall–runoff relationship: an Australian perspective. Water Resour Res 51:2444–2463

Sinclair Knight Merz (2010) Developing guidelines for the selection of streamflow gauging stations. Sinclair Knight Merz, Malvern. www.bom.gov.au/water/hrs/references.shtml

Smith I, Syktus J, Rotstayn J, Jeffrey S (2013) The relative performance of Australian CMIP5 models based on rainfall and ENSO metrics. Aust Met Ocean J 63:205–212

Taylor KE, Stouffer RJ, Meehl GA (2012) An overview of CMIP5 and the experiment design. Bull Am Meteorol Soc 93:485–498

Timbal B (2009) The continuing decline in South-East Australian rainfall — update to May 2009. CAWCR Res Lett 2:1–8

Timbal B, Fawcett R (2013) An historical perspective on South Eastern Australia rainfall since 1865. J Clim 26: 1112–1129

Timbal B, McAvaney BJ (2001) An analogue-based method to downscale surface air temperature: application for Australia. Clim Dyn 17:947–963

Timbal B, Fernandez E, Li Z (2009) Generalization of a statistical downscaling model to provide local climate change projections for Australia. Environ Model Softw 24:341–358

Timbal B, Griffiths M, Tan KS (2015a) Rainfall and streamflow in Greater Melbourne catchment area: variability and recent anomalies. Clim Res 63:215–232

Timbal B, Abbs D, Bhend J, Chiew FHS and others (2015b) Murray–Darling cluster report. In: Ekstrom M, Whetton P, Gerbing C, Grose M, Webb L, Risbey J (eds) Climate change in Australia — projections for Australia's natural resource management regions: cluster reports. CSIRO and Bureau of Meteorology, Melbourne. www.climatechangeinaustralia.gov.au/media/ccia/2.1.6/cms_page_media/172/MURRAY_BASIN_CLUSTER_REPORT_1.pdf

Turner M, Bari M, Amirthanathan G, Ahmad Z (2012) Australian network of hydrologic reference stations — advances in design, development and implementation. 34th Hydrology and Water Resources Symposium. Engineers Australia, Sydney, p 1555–1564

van Vuuren DP, Edmonds J, Kainuma M, Riahi K and others (2011) The representative concentration pathways: an overview. Clim Change 109:5–31

von Storch H, Zwiers FW (2004) Statistical analysis in climate research. Cambridge University Press, Port Melbourne

Weller E, Cai W (2013) Realism of the indian ocean dipole in CMIP5 models: the implications for climate projections. J Clim 26:6649–6659

Editorial responsibility: Gerrit Hoogenboom, Gainesville, Florida, USA

Submitted: January 22, 2016; Accepted: December 1, 2016
Proofs received from author(s): January 24, 2017